Extracellular Recordings of Field Potentials from Single Cardiomyocytes

Norbert Klauke,* Godfrey L. Smith,† and Jon Cooper*
*Department of Electronics, University of Glasgow, Glasgow G12 8LT, United Kingdom; and †Institute of Biomedical and Life Sciences, University of Glasgow, Glasgow G12 8QQ, United Kingdom

ABSTRACT Open microfluidic channels were used to separate the extracellular space around a cardiomyocyte into three compartments: the cell ends and a central partition (insulating gap). The microchannels were filled with buffer solution and overlaid with paraffin oil, thus forming the cavities for the cell ends. The central part of the cardiomyocyte rested on the partition between two adjacent microchannels and was entirely surrounded by the paraffin oil. This arrangement increased the extracellular electrical resistance to >20 MΩ and facilitated the recording of the time course of the change in extracellular voltage and current during subthreshold and suprathreshold stimuli. The waveform of the extracellular current and voltage in response to an extracellular depolarizing stimulus comprised an initial monophasic signal followed by a biphasic signal with a delay of 2–15 ms. The latter was associated with a transient contraction and therefore caused by an action potential. The biphasic signal became monophasic after the depolarization of one cell end by raised extracellular [K^+]. This form of differential recording revealed the repolarization phase of the action potential. At rest, the sarcomere length within the gap was 12% ± 4.8% longer than outside the gap, but intracellular Ca^{2+} transients occurred to the same extent as that observed in the outer pools. This data demonstrate the feasibility of the use of a microfluidic bath design to limit the extracellular resistance between two ends of an isolated cardiomyocyte.

INTRODUCTION

Previously, automated electrophysiology in microchip-based systems technology has emerged as a method for producing a high throughput alternative to traditional glass electrode single cell patch clamp techniques (1). Using such devices, it has already been shown that small cells with smooth surfaces will readily seal against the arrays of microfabricated apertures, resulting in a patch on a chip technology. However, the irregular shape and surface structure of primary cells, such as nerve cells and myocytes, has thus far prevented the formation of a high-resistance seal on this existing class of fabricated apertures, excluding their use in an automated high throughput voltage/current clamp (2).

Electrically excitable cells, like adult ventricular myocytes, display a negative transmembrane potential of ~−85 mV at rest which transiently depolarizes upon threshold stimulation due to the influx of cations, e.g., sodium and calcium (an event known as the action potential). The action potential is initiated at a membrane patch and propagates along the cell surface through local circuit activation. Extracellular electrodes can report the extracellular current flow as a biphasic signal if the gap between the electrode surface and the cell surface is sufficiently small, e.g., <10 nm.

We describe a soft-lithographic microfluidic structure for the exploration of heart electrophysiology, which enables extracellular voltages and currents to be measured with extracellular electrodes which are not in contact with the cell. The structure of the microchannels was formed by micromolding in a polymer film and contained lithographically patterned planar microelectrodes for cardiomyocyte stimulation and extracellular electrical recording. An additional fabrication step was used to form an insulating polymer partition (gap), which served to define two microfluidic pools within the microchannel, reminiscent of the sucrose gap technique (3). This latter structure enabled the two ends of the myocyte to be physiologically manipulated independently of each other. Single adult ventricular myocytes were aligned within the device, bridging two microfluidic pools, and lying across the lithographically defined electrically insulating polymer partition (or gap). We show how this electrical separation of the two ends of the cell offers a means to record single cell extracellular potentials and currents during the course of an action potential. The seal resistance, measured across the cell between the two microfluidic pools, was >20 MΩ. The cell was electrically stimulated across this insulating gap and the recorded extracellular currents and voltages were related to the size and duration of the trigger pulse. Simultaneously, the effect of the insulating gap on the e-c coupling was also investigated, by measuring sarcomere length and Ca^{2+} transients at different rates of extracellular pacing. Make-stimulation was found to occur at voltage pulses more than 10% above threshold, whereas break-stimulation occurred between 1% and 10% above that threshold.

METHODS

Cell isolation

Experiments were performed in enzymatically isolated rabbit ventricular myocytes. Hearts were removed from terminally anaesthetized rabbits (1 mg kg^{-1} euthatol). Myocytes were isolated from the left ventricle by perfusion with collagenase solution (4) and kept in base Krebs solution containing

Submitted March 16, 2006, and accepted for publication June 30, 2006.

Address reprint requests to Norbert Klauke, E-mail: norbert@elec.gla.ac.uk.

0006-3495/06/10/2543/09 $2.00

doi: 10.1529/biophysj.106.085183

120 mM NaCl, 20 mM sodium *N*-hydroxyethylpiperazine-*N*′−2-ethane sulphonic acid, 5.4 mM KCl, 0.52 mM NaH_2PO_4, 3.5 mM $MgCl_2$, $6H_2O$, 20 mM taurine, 10 mM creatine, 11.1 mM glucose, 0.1% bovine serum albumin, 0.1 mM $CaCl_2$, pH adjusted to 7.4 with 100 mM NaOH. Unless otherwise stated, all chemicals were obtained from Sigma-Aldrich (Gillingham, UK).

Cell positioning

Single isolated ventricular myocytes, which were suspended in buffer solution and placed on top of the microchannels, were directed into the microchannel through the repellent force of the hydrophobic poly(dimethylsiloxane) (PDMS) surface. To span the gap between two adjacent microwells a single cardiomyocyte was guided along the channel toward the barrier dams and rested on top of the dams between the adjacent microchannels. The excess of buffer around the cell was removed and the mineral oil was allowed to contact the PDMS of the gap region, thus entirely surrounding the central part of the cell. The low viscosity of the insulating mineral oil enabled it to fill the microcavities on the irregular-shaped cardiomyocyte. The thickness of the remaining aqueous layer between the cell surface and the oil was variable but <50 nm, giving rise to a seal resistance of ~20 MΩ.

Fabrication protocol

The microchannels and microelectrodes were fabricated as described previously by us (5). Microfluidic channels with a 20- or 40-μm gap were molded into 12–15-μm-thick films of the polymeric elastomer, PDMS, which was sealed against a planar array of stimulating-recording microelectrodes. The PDMS was rendered hydrophobic by an overlayer of paraffin oil before the cardiomyocytes were laid across the gap between two adjacent microchannels. In the majority of cases, unless stated, extracellular recordings and cell stimulation were carried out using a pair of 20-μm microlithographically patterned nonpolarizable, reversible Ag|AgCl electrodes, each positioned 90 μm from the insulating gap. For reasons of comparison, cells were also stimulated and extracellular currents and voltages were recorded using a microfabricated nonreversible, polarizable gold electrode pair. The main source of capacitative decay in response to a voltage step was identified as the integrated microelectrodes (independent of the electrode material). The capacitance with a heart cell in place across the oil gap was measured to 15 pF using a Thandar TC200 digital LCR meter.

Stimulation protocol

The stimulus voltage strength was gradually raised to threshold and maintained at ~10% above threshold to delay the takeoff and thus keep the signal temporally separate from the stimulus artifact (break stimulation, see Fig. 3). A rectangular voltage pulse (~0.1 V) was applied either at 0.5 Hz or 1.0 Hz for ~3 ms (for current measurement) or for ~50 μs (for voltage measurement). An offset of ±100 mV was used to adjust the range of the differential amplifier (~280 gain, 0–8.35 mV range).

A custom built constant current supply (0–10 nA, rectangular pulses of both polarities) was used to measure the seal resistance. The pulse amplitude was raised until the electrical capacitance (~15 pF) of the lithographic gap was charged and the voltage reached the steady state. From the voltage/current ratio a seal resistance of >20 MΩ was calculated.

The extracellular electrical signals were recorded with a voltage clamp amplifier (EPC-7, List) or custom built amplifiers, comprising an operational amplifier for the current measurement and a differential amplifier for the voltage measurement. Analog signals were digitized at 20 kHz (current) or 1 kHz (voltage) using a National Instruments (Austin, TX) A/D card and custom designed software. A monophasic extracellular voltage and a monophasic extracellular current were first recorded at subthreshold stimulation. This was then followed by biphasic signals (after the transition toward threshold stimulation). The time delay between the monophasic and the biphasic signals ranged from 2–15 ms.

Optical measurements

The simultaneous recording of electrical and optical activity required the fabrication of the microfluidic device on a transparent substrate. We chose to use a thin microscope coverslip (No. 1) to enable the use of high numerical aperture objective lenses, e.g., the water immersion 63× C-Apochromat (1.2 numerical aperture, Zeiss, Jena, Germany). Intracellular calcium was imaged in Fluo-3 loaded cardiomyocytes with 60 frames/s, and sarcomere length changes were recorded with 150 frames/s (IonOptix, Milton, MA) as described (5). To reduce movement artifacts, the fluidic content of the two pools was lowered until the free moving cell ends were gently pressed onto the glass surface (Fig. 1 *D ii*, *iii*).

RESULTS

Extracellular recordings of the electrical activity have been used in the past to obtain information concerning the process of the myocyte's activation, e.g., the propagation of the action potential in multi-cellular preparations (6). Under normal circumstances, the amplitude of extracellular potential, recorded using an extracellular electrode, is inherently small (~100 μV), due to the voltage drop in the bulk of the buffer solution around the cell (7–9). By introducing an increased electrical resistance between the two measurement microelectrodes within the microfluidic chambers, we have developed a method which has enabled us to increase this measured output voltage/current signal. The electrical seal and the microfabricated hydrophobic gap both form a diffusion barrier which splits the extracellular space around the cell, producing two microfluidic compartments, with a limited diffusional cross talk between them.

Fabrication and operation of the gap

Arrays of parallel microchannels (40-μm wide, 12–15-μm high, 1000-μm long, 70-μm pitch) with integrated planar microelectrodes (40 × 20 μm) were fabricated on microscope coverslips (Fig. 1 *A*). The microchannels in the arrays were aligned along their longitudinal axis with a 20- or 40-μm-wide gap between adjacent channels (Figs. 1 *A* and 2 *A*). The microchannels were filled with saline solution and overlaid with paraffin oil to prevent evaporation of the buffer solution. Apart from that, the oil was crucial to the formation of the seal. In comparison to the saline solution, it has a higher affinity to the PDMS film, which made it stick to the polymer surface, including the gap, whereas the aqueous buffer solution was forced into the channel cavity. A functional microfluidic structure comprised a pair of microchannels with the 20- or 40-μm gap between them and the pair of integrated electrodes. The extracellular electrodes were used for both electrical stimulation and recording of the voltage/current response. A path for current flow was provided after a ventricular myocyte was laid across the lithographic gap (Fig. 1 *B*). The cardiac myocyte touched both edges of the gap but not the floor so that the mineral oil was able to form a collar around the central part of the cell, which then appeared constrained (Fig. 1 *C*). The sarcomere length within the gap

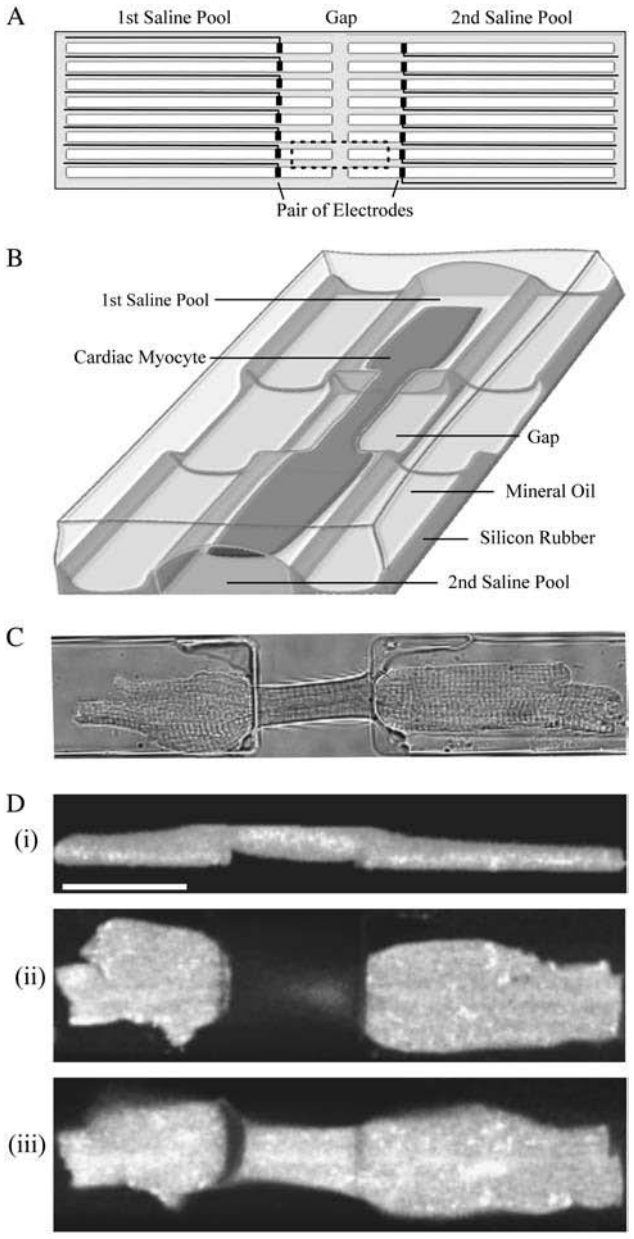

FIGURE 1 (*A*) Sketch outlining the array of microchannels and integrated microelectrodes. (*B*) Illustration of the area indicated in *A* with a cardiac myocyte laid across the insulating gap. (*C*) Micrograph (transillumination) of an adult ventricular myocyte laid across a 40-μm-wide gap. (*D*) Reconstructed z-stack (*i*) of a Fluo-3 loaded cardiac myocyte and individual optical slices at ~1 μm (*ii*) and ~4 μm (*iii*) above the glass surface. Calibration bar, 40 μm.

was not significantly different (112% ± 4.5%) from the sarcomere length at the distal and proximal ends of the cell. Thus, the forces stretching or compressing the segment of the myocytes within the gap were not sufficient to produce significant changes in sarcomere length. Confocal z-sections show the cell ends in intimate contact with the glass surface of the coverslip, whereas the central part of the cardiomyocyte was supported by the gap structure (Fig. 1 *D*). Individual confocal slices (not shown) indicate that the cell height increases in the oil gap such that the cell's cross-sectional area remains approximately constant.

Fig. 2 shows three different gap configurations, which were used to investigate the electrical current in response to rectangular voltage pulses. The two current spikes at the onset and offset of the stimulus were caused by the capacitive charging of the electrode and were common to all three configurations (Fig. 2 *B*). As described in the Methods, the source of the capacitive decay was the polarization of the integrated electrodes and amounts to ~15 pF, giving a time constant of ~0.3 ms. In the absence of any ionic continuity between the two pools, no steady-state current was observed (Fig. 2, *A i* and *B i*). Bridging the gap with a glass rod established the ionic continuity between the two pools and caused a slowly decaying current according to the amplitude of the voltage pulse (Fig. 2, *A ii* and *B ii*). The origin of the slow capacitative decay is unknown but may reside in the gap region where a thin layer of water is sandwiched between the glass rod and the surrounding oil. Finally, in the presence of a cardiomyocyte, a biphasic current signal appeared in response to suprathreshold stimulation (Fig. 2, *A iii* and *B iii*). The resistance to current flow between the two microfluidic pools, offered by the gap with the cell in place, was measured as having a value of >20 MΩ, using the voltage response to constant current pulses (data not shown).

Electrical stimulation across the gap

In the absence of the gap, a voltage pulse of ~600-mV amplitude and 2-ms duration applied to a pair of planar microelectrodes 200 μm apart was sufficient to stimulate a ventricular myocyte confined in a microchannel (5). The electrical seal generated in the barrier gap reduced the threshold for electrical stimulation to <100 mV as measured in this study with the constant voltage stimulator (Fig. 2 *B*).

When the amplitude of the voltage pulse was incrementally raised to threshold and maintained at ~10% above threshold, a biphasic electrical signal appeared within <15 ms after the end of the stimulus. The cellular signal was obtained by background subtraction of the stimulus artifact (Fig. 3, *A* and *B*, *insets*). Successful electrical stimulation was evidenced by the simultaneous measurement of cell shortening and calcium transients (Figs. 4 and 5). Excitation-contraction coupling (e-c coupling) was normal in every part of the cell including the gap, as revealed by line scan imaging of Fluo-3 (provided as online supplementary data), further demonstrating the lack of effect of forces stretching or compressing the myocytes within the gap.

Extracellular waveforms during the stimulated action potential

Control current and voltage signals were recorded at subthreshold stimulation. These signals were then subtracted from the waveforms recorded during stimulated action

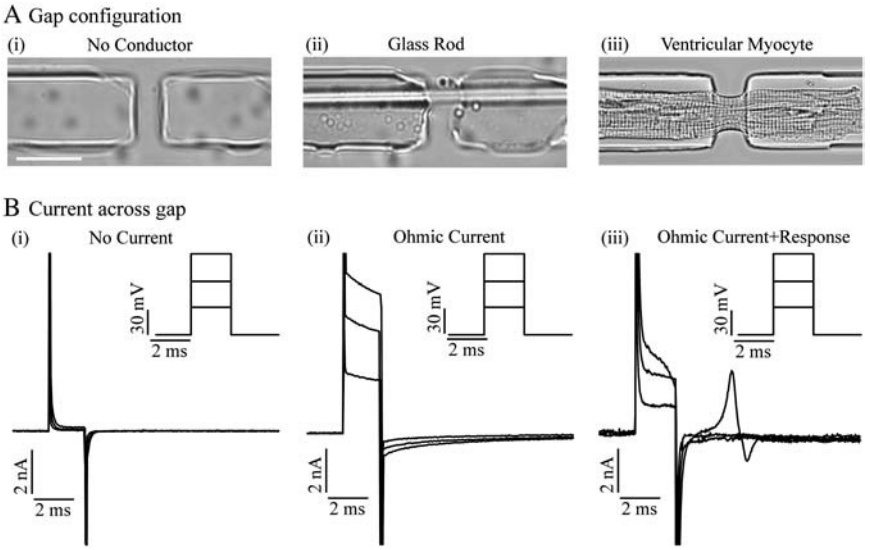

FIGURE 2 Micrographs of three gap configurations (*A*) and the corresponding current response (*B*) to rectangular monophasic voltage pulses applied across the lithographic gap without a conductor (*i*), with a glass rod (*ii*), and with an isolated ventricular myocyte (*iii*). Note the biphasic current response evoked at suprathreshold stimulation of the ventricular myocyte (*B iii*).

potentials as indicated through the associated cell contractions. After background subtraction, the upstroke, plateau, and the repolarization of the underlying action potential could all be identified on the voltage recording (field potential, Fig. 3 *A i*, *1–3*), whereas the current recording was flat apart from the upstroke (Fig. 3 *B i*, *1*). The high frequency, high amplitude biphasic extracellular voltage during the upstroke generated a biphasic extracellular current (Fig. 3 *B i*), whereas the low frequency, low amplitude extracellular voltage during the plateau and repolarization failed to evoke detectable extracellular currents.

The two phases during the upstroke could reflect the temporally separate depolarizations of the cell ends, causing two current/voltage transients of opposite polarity. The electrical resistance within the gap enabled the detection of the time course and amplitude of the depolarization traveling from one end of the cell to the other. The inactivation of one cell end caused the loss of one phase (Fig. 6), generating a monophasic action potential similar to an injury potential (10). Importantly, the seal did not impair the electrotonic spread of the activation itself.

Extracellular waveforms during the subthreshold to threshold transition

By organizing the electrochemical configuration of the stimulating electrodes, with respect to each other (using one as a pseudoreference), the gap could be used to depolarize one cell end with respect to the other end. This enabled, for the first time to our knowledge, the recording of the extracellular voltage and current at subthreshold stimulation and the analysis of the transition toward threshold stimulation (Fig. 3, *A ii* and *B ii*).

First, a monophasic extracellular voltage and a monophasic extracellular current were recorded at subthreshold stimulation together with the stimulus artifact (Fig. 3, *A*ii and *B*ii,*). The inset shows the subtracted transients. This was then followed by biphasic signals (after the transition toward threshold stimulation) with the associated cell contraction. The time delay between the monophasic and the biphasic signals was $<$15 ms but disappeared when the stimulus strength was $>$30% above threshold (the so-called ''make stimulation'', data not shown). The monophasic extracellular voltage/current signal during the trigger phase (Fig. 3, *A ii* and *B ii*, *open circle*) indicated the depolarization of one cell end and was never associated with contraction.

In situations when the passive impulse from the depolarized cell end was strong enough to spread to the distal side of the gap, a biphasic signal was recorded with a delay of 2–15 ms. The delay could reflect the time needed to charge the capacitance of the system ($\sim$15 pF) comprising the cell capacitance and the capacitance generated in the interface between the oil and the cell surface. The second phase of the biphasic signal was normally smaller compared to the first phase (Fig. 3, *A ii* and *B ii*).

Extracellular waveforms, cell shortening, and calcium transients

The microfluidic gap structure was used to monitor simultaneously the excitation of adult ventricular myocytes both optically and electrically (Figs. 4 and 5). The extracellular current signal was correlated with the cell shortening at threshold and suprathreshold stimulation (Fig. 4 *A*) and at stimulation rates of 0.5 Hz and 1.0 Hz, respectively (Fig. 4 *B*). The amplitude of the cell shortening increased during the first $\sim$10 beats of any train of cell contractions, a commonly observed ''positive staircase'' in isolated cardiac myocytes indicating the filling of the calcium stores (Fig. 4 *A*). In contrast, the amplitude of the corresponding current record

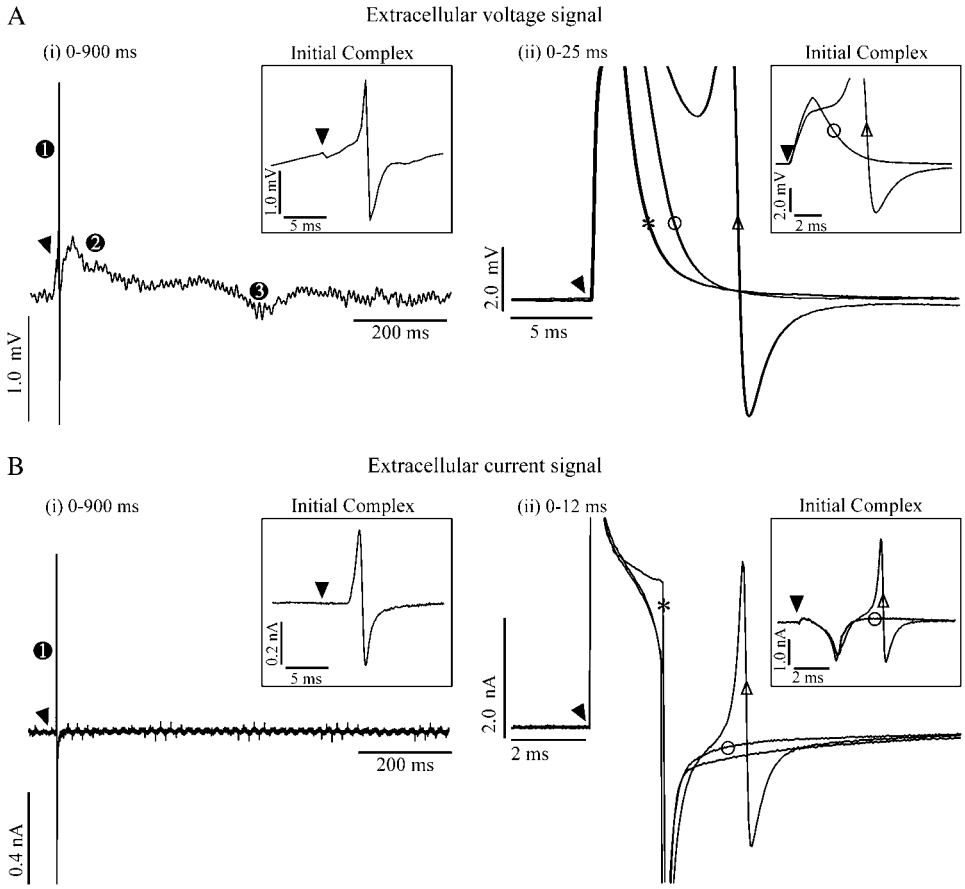

FIGURE 3 Recordings of the extracellular voltage (*A*) and extracellular current (*B*) during a stimulated action potential. The background subtracted traces on the left (*A i* and *B i*) enclose the three phases of the action potential, namely the upstroke (*1*), plateau (*2*), and repolarization (*3*). Note the absence of the last two phases on the current record (*B i*). Insets focus on the initial biphasic complex. The traces on the right (*A ii* and *B ii*) include the stimulus artifact. The trigger phases at subthreshold (○) and threshold (△) and the background (*) are shown at high time resolution. The insets show the background subtracted initial complex, again at subthreshold (○) and threshold (△) stimulation. Arrowheads indicate the arrival of the trigger pulse.

declined, and the delay of the biphasic signal increased until a steady state was reached (Fig. 4 *A ii*). The data of the simultaneous recordings of the extracellular current and the cell shortening are summarized in Table 1.

At higher frequency stimulation (1.0 Hz), the amplitude of the cell shortening decreased together with the amplitude of the extracellular current (Fig. 4 *B*). The cardiac myocyte adapted to the frequency change from beat to beat (Fig. 4 *B ii*, *inset*).

In a further set of experiments, the cells were electrically paced using the extracellular electrodes by progressively increasing the potential from a value which was subthreshold to one which was suprathreshold. Extracellular voltages were measured at the microelectrodes, while, at the same time, the intracellular calcium transients were measured fluorescently (Fig. 5). The positive staircase of the calcium trace at the beginning of the suprathreshold stimulation reflects the Ca^{2+} loading of the sarcoplasmic reticulum (Fig. 5 *A i*). It was noted that the negative phase of the voltage signal was associated with the stimulus artifact (Fig. 5 *A ii*), while an additional positive phase of the voltage signal was observed when a calcium transient occurred, indicating an action potential.

We then measured an action potential duration of ~400 ms at 0.5 Hz and 1.0 Hz (Fig. 5 *B ii*). The amplitude of the calcium transient increased at the higher pacing rate but the duration decreased (Fig. 5 *B i*). Examination of the extracellular voltage showed that the repolarization was clearly detectable after averaging at least 10 action potentials (Figs. 3 *A i* and 5 *B ii*). The amplitude of the plateau was <0.5 mV, and its magnitude throughout the experiments remained constant, indicating that both cell ends depolarized to the same level during an action potential.

Differential microfluidic manipulation of the cell ends

Finally, to investigate whether the two ends of the cell could be ionically isolated from each other, it was necessary to show that the lithographic gap created a barrier that could prevent ionic diffusion. By using a micropipette, positioned within one of the adjacent microfluidic channels, we added a fluorescent dye, fluoresceine, and showed that the lithographic gap was able to obstruct the diffusion of the fluorochrome between the two pools (Fig. 6 *A*). In a second (separate) series of experiments, we then increased the potential difference between the cell ends by raising the extracellular potassium concentration in one pool to 10 mM (Fig. 6 *B*). The elevated potassium around one cell end prevented its excitation, so that the extracellular current signal changed from a biphasic to a monophasic transient (Fig. 6 *B i*,

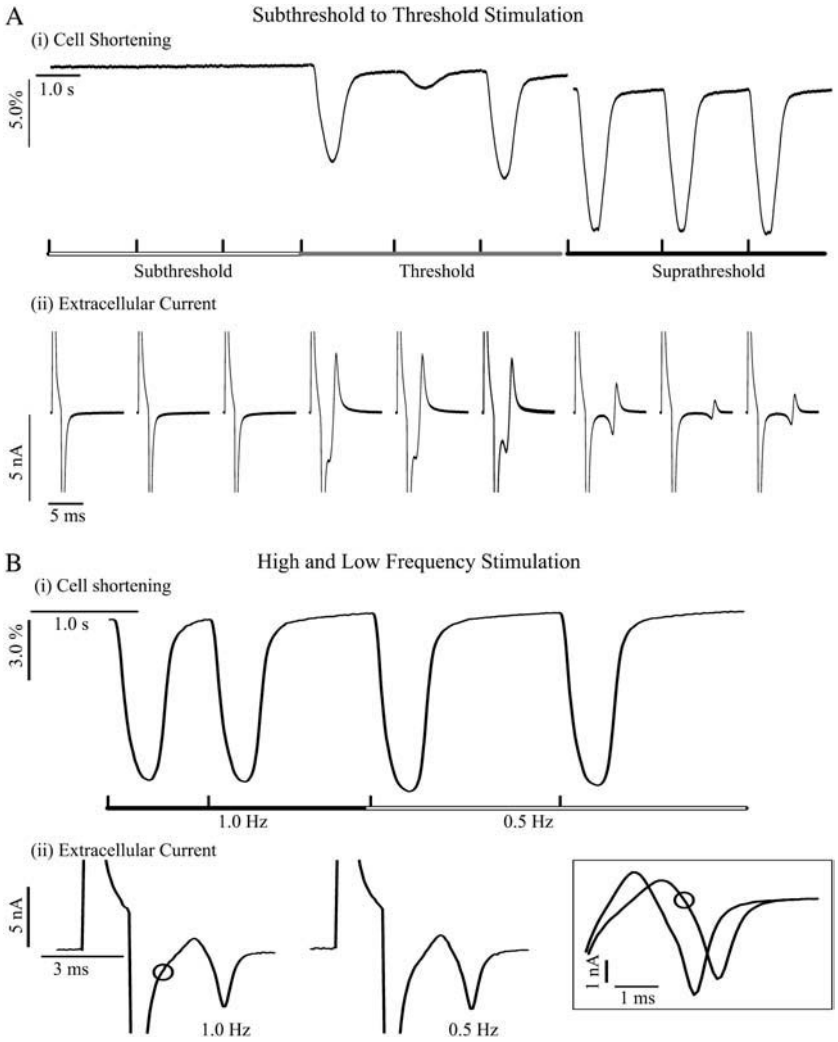

FIGURE 4 Simultaneous recordings of the cell shortening (*A i*) and the extracellular current (*A ii*) before and after threshold stimulation and at 0.5 Hz and 1.0 Hz (○) stimulation, respectively (*B*). Note the beat to beat adaptation of the current response to the frequency change (Fig. 4 *B ii*, *inset*).

asterisk). The extracellular voltage signal increased in size (>2 mV) and showed a sustained plateau (Fig. 6 *B ii*, *asterisk*). This signal reflected the time course of the action potential, application of the drug cisapride (10 μM) caused a prolongation of the monophasic signal (Fig. 6 *B iii*).

DISCUSSION

Optical and electrical measurements from cell populations have been developed independently of each other, particularly in systems where there has been a need to increase the throughput of test compounds in the screening laboratory (1,2). Simultaneous recordings of electrical and optical data (11,5) have become standard practice in electrophysiological experiments, revealing details which single parameter measurements alone would not (for example, the effect of L-type calcium channel modulators (12) on downstream calcium release events). The combined recording of electrical and optical signals has not been implemented into cell-based assays for ion channel activity. Here we demonstrate the simultaneous monitoring of the electrical and mechanical activity in isolated adult ventricular myocytes in microfluidic formats.

Insulating gap with fluidic sealant

To date, extracellular measurements to detect the extracellular voltage change using planar microelectrodes have required that the metal interface be in close contact with the cell surface, thus generating a high extracellular electrical resistance (7). The extracellular voltage originates from the transmembrane potential, which generates current across the membrane resistance and the extracellular resistance, resulting in a voltage divider relation: the higher the extracellular electrical resistance, the higher the amplitude of the extracellular signal. For example, in cell cultures grown on microelectrode arrays, the amplitude of the extracellular field potential is <5 mV due to the ~10-nm gap between the cell surface and the electrode surface (8).

The irregular and highly structured form of the membrane of the adult ventricular myocyte prevents any close (<50 nm)

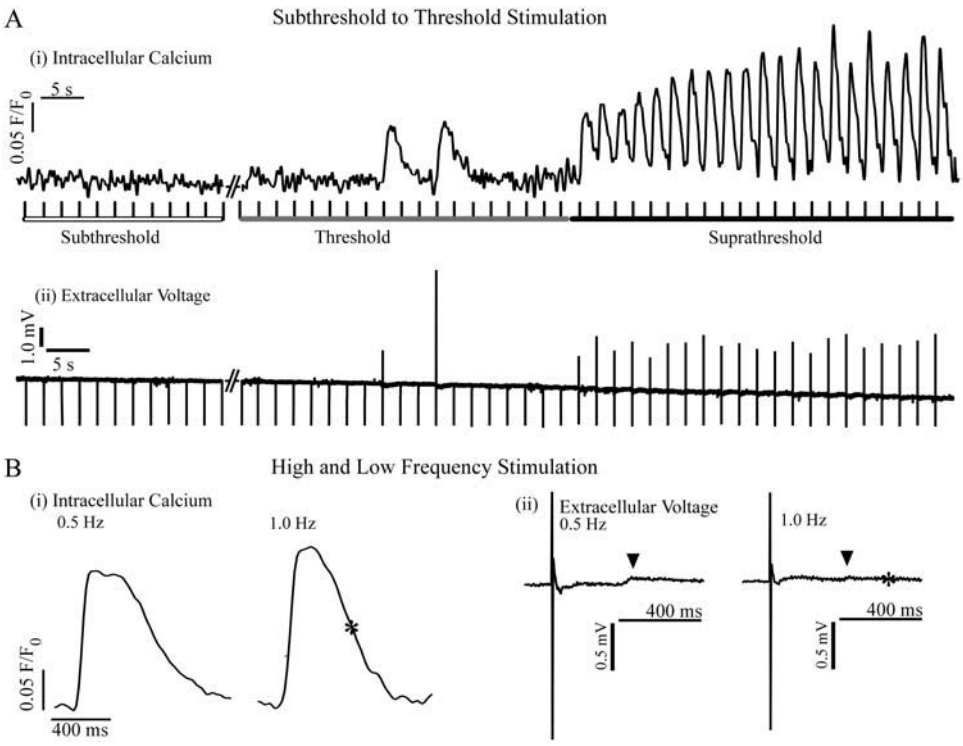

FIGURE 5 Simultaneous recordings of the intracellular calcium concentration (*A i*) and the extracellular voltage (*A ii*) before and after threshold stimulation and at 0.5 Hz and 1.0 Hz (*) stimulation (*B*). The arrowheads on the voltage traces (average of 10 traces) indicate the repolarization (*B ii*).

contact with a planar microelectrode, and as a consequence, signal amplitudes that have been recorded (13) have been very small (typically $<100\ \mu$V). In this work, we have described a new lithographic format, in which the cell is partitioned into two microfluidic pools, with each end being separated by a high impedance gap based on a fluidic sealant (paraffin oil).

The extracellular potentials, recorded with planar microelectrodes from isolated cardiomyocytes laid across the insulating gap, reached ~3-mV amplitude, comparable to previous work with cultured cells (8) but without the need for a close contact between the cell and the electrode surface. The extracellular waveforms described in this work (Fig. 3, *A* and *B*) resemble the field potentials recorded with microelectrode arrays in cardiac cell culture (8,9) or those of single microelectrodes on multi-cellular preparations (6,14).

Monophasic waveform at subthreshold stimulation

In a space-clamped cardiac myocyte, the membrane potential changes uniformly in response to the current injection. In contrast, electrically stimulated cardiac myocytes are exposed to a highly nonuniform electric field and the cell ends experience the opposing polarity most when the longitudinal axis is aligned to the electric field (15). This arrangement shifts the transmembrane potential from rest toward opposite directions, as shown with optical recordings from multiple sites along the cell's longitudinal axis (16). The presence of a high extracellular resistance, a feature of the insulating gap of our new configuration, allowed for the repeated transient depolarization of one cell end below threshold whereas the other end was kept at ground potential. The associated extracellular current and voltage signal was monophasic and appeared within 1 ms after the make of the rectangular stimulus (<40 mV amplitude) but decayed immediately after the break of the voltage pulse (Fig. 3, *A* and *B*). This nonregenerative behavior could represent the electrotonic displacement of the membrane potential through inward currents activated during subthreshold stimulation. No contraction or change in intracellular calcium was observed in any region of the cell in these circumstances. As recently shown in a guinea pig ventricular model cell electrically stimulated at low field strengths (~5 V/cm), the cathode-facing cell end produces an inward-directed sodium current spike. This transient current works synergistically with the inward potassium current at the anode-facing cell end to bring the membrane potential to threshold (17).

Biphasic waveform at suprathreshold stimulation

Cell excitation occurs when the sum of the ionic currents along the cell length produces a net inward current that raises the intracellular potential above threshold (17). According to the cable theory, the electrically active area of the membrane then travels along the longitudinal axis of the preparation and generates a biphasic (voltage) signal after crossing the recording electrode (18). This biphasic waveform, as a measure of

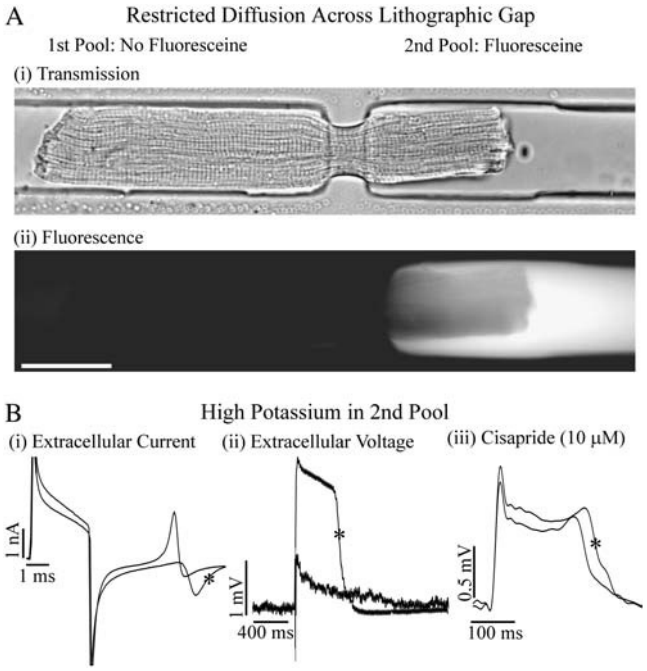

FIGURE 6 (*A*) Transmission and fluorescence micrograph of a cardiomyocyte laid across the insulating gap. The gap seals the cell ends against each other as shown by the limited diffusion of fluoresceine added to the second pool (Fig. 6 *A ii*). Calibration bar, 40 μm. (*B*) The diffusion barrier was used to depolarize one cell end in raised potassium (10 mM). Under these conditions, the biphasic waveform of the extracellular current turned monophasic (Fig. 6 *B i* *). The extracellular voltage signal increased in amplitude and comprised a pronounced plateau phase (Fig. 6 *B ii* *). The need for a potassium bias to reveal the repolarization on extracellular field potentials has been reported in cardiac myocytes from the frog (24). Within 20 s after the addition of 10 μM cisapride to the intact cell end, the action potential duration increased ~30 ms (Fig. 6 *B iii*).

the extracellular potential during the takeoff, has previously been related to the second derivative of the transmembrane potential (7). In the case of a single cardiac myocyte electrically stimulated across the microfluidic gap, the depolarization of the membrane propagates through local circuits on the cell surface across the gap. Since the recording electrode is fixed on one side of the gap, the extracellular electrical signal comprises two phases of opposite polarity (Fig. 3).

TABLE 1 Extracellular current and cell shortening

	Current	Shortening
Amplitude	1.5 ± 0.2 nA	9.62% ± 0.012%
Rise time	2.38 ± 0.27 ms	499 ± 29 ms
Decay time	0.35 ± 0.91 ms	504 ± 154 ms

Adult ventricular myocytes ($n = 5$) were field stimulated at 0.5 Hz and the extracellular current was recorded together with cell shortening (measured as sarcomere length changes). Records were taken 30 s after the onset of stimulation (rise time = time to rise to half maximum, decay time = time to return to 10% of maximum, mean ± SE). Current parameters were analyzed for one phase only.

The biphasic signal was always associated with cell contraction (Figs. 4 and 5).

Microfluidic manipulation of cell ends

The insulating gap described in this work was tested as a diffusion barrier for small molecules or ions, e.g., fluoresceine and potassium, and prevented the mixing of the different solutions around the cell ends (Fig. 6). This technique was then used to examine the effect of the selective depolarization of one cell end on the extracellular electrical signal. We observed an ~3-fold increase in amplitude of the voltage signal, allowing the unambiguous identification of the repolarization phase, which was less obvious on extracellular potential records of noninjured cells (Fig. 5 *B*). This modification allowed the effects of a potassium channel blocker cisapride (19) to be observed as a prolongation of the action potential duration (Fig. 6 *B iii*). Other techniques to control the extracellular space use laminar flow to prevent the mixing of two microstreams directed toward isolated cardiomyocytes but are difficult to combine with electrical recordings (20).

Related electrophysiological techniques

The lithographic gap described in this work is analogous in its function both to the sucrose gap used in multi-cellular cardiac preparations (3,21) and to the oil seal, used to keep the intracellular solution around the skinned end of a ventricular myocyte separate from the extracellular solution around the intact end during voltage clamp (22).

In contrast to these previous techniques, the lithographic gap is experimentally simpler and has the potential to be scaled using standard lithographic methods to develop a high throughput electrophysiological format for primary cells. Such a system is made analytically more powerful due to the fact that the extracellular electrodes cannot only be used to stimulate the cell (at different rates, for example) but can also detect the difference between the potential inside and outside of the cell. We have shown that the insulating gap can be used to manipulate the extracellular environment of the cell ends independently (Fig. 6). This technique enables the generation of extracellular and intracellular gradients of chemicals, e.g., ions or drugs, and the electrical and optical detection of their effect on the cardiomyocyte behavior (23).

SUPPLEMENTARY MATERIAL

An online supplement to this article can be found by visiting BJ Online at http://www.biophysj.org.

The authors thank the Engineering and Physical Sciences Research Council, Biotechnology and Biological Sciences Research Council, and Medical Research Council, who funded this work as part of the IRC in Bionanotechnology. Support from British Heart Foundation funding to G.L.S. is acknowledged.

REFERENCES

1. Falconer, M., F. Smith, S. Surah-Narwal, G. Congrave, Z. Liu, P. Hayter, G. Ciaramella, W. Keighley, P. Haddock, G. Waldron, and A. Sewing. 2002. High-throughput screening for ion channel modulators. *J. Biomol. Screen.* 7:460–465.
2. Wood, C., C. Williams, and G. J. Waldron. 2004. Patch clamping by numbers. *Drug Discov. Today.* 9:434–441.
3. Reuter, H. 1979. Properties of two inward membrane currents in the heart. *Annu. Rev. Physiol.* 41:413–424.
4. Eisner, D. A., C. G. Nichols, S. C. O'Neill, G. L. Smith, and M. Valdeomillos. 1989. The effects of metabolic inhibition on intracellular calcium and pH in isolated rat ventricular cells. *J. Physiol.* 411: 393–418.
5. Klauke, N., G. L. Smith, and J. Cooper. 2003. Stimulation of single isolated adult ventricular myocytes within a low volume using a planar microelectrode array. *Biophys. J.* 85:1766–1774.
6. Vaughan Williams, E. M. 1959. Relation of extracellular to intracellular potential records from single cardiac muscle fibres. *Nature.* 183: 1341–1342.
7. Kovacs, G. T. A. 2003. Electronic sensors with living cellular components. *Proc. IEEE.* 91:915–929.
8. Meyer, T., K.-H. Boven, E. Günther, and M. Fejtl. 2004. Microelectrode arrays in cardiac safety pharmacology. A novel tool to study QT interval prolongation. *Drug Saf.* 27:763–772.
9. Halbach, M. D., U. Egert, J. Heschler, and K. Banach. 2003. Estimation of action potential changes from field potential recordings in multicellular mouse cardiac myocyte cultures. *Cell. Physiol. Biochem.* 13:271–284.
10. Franz, M. R. 1999. Current status of monophasic action potential recording: theories, measurements and interpretations. *Cardiovasc. Res.* 41:25–40.
11. Bers, D. M. 2001. Excitation-Contraction Coupling and Cardiac Contractile Force. Kluwer Academic Publishers, Dordrecht, The Netherlands.
12. Inoue, M., and J. H. B. Bridge. 2003. Ca^{2+} sparks in rabbit ventricular myocytes evoked by action potentials. Involvement of clusters of L-type Ca^{2+} channels. *Circ. Res.* 92:532–538.
13. Werdich, A. A., E. A. Lima, B. Ivanov, I. Ges, M. E. Anderson, J. P. Wikswo, and F. J. Baudenbacher. 2004. A microfluidic device to confine a single cardiac myocyte in a sub-nanoliter volume on planar microelectrodes for extracellular potential recordings. *Lab Chip.* 4:357–362.
14. Spach, M. S., R. C. Barr, G. A. Serwer, J. M. Kootsey, and E. A. Johnson. 1972. Extracellular potentials related to intracellular action potentials in the dog purkinje system. *Circ. Res.* 30:505–519.
15. Knisley, S. B., and A. O. Grant. 1995. Asymmetrical electrically induced injury of rabbit ventricular myocytes. *J. Mol. Cell. Cardiol.* 27:1111–1122.
16. Sharma, Y., and L. Tung. 2002. Spatial heterogeneity of transmembrane potential responses of single guinea-pig cardiac cells during electric field stimulation. *J. Physiol.* 542:477–492.
17. Sharma, V., R. C. Susil, and L. Tung. 2005. Paradoxical loss of excitation with high intensity pulses during electric field stimulation of single cardiac cells. *Biophys. J.* 88:3038–3049.
18. Sperelakis, N. 2001. Cell Physiology Source Book. A Molecular Approach. Academic Press, San Diego, CA.
19. Dumotier, B. M., M. Bastide, and M. M. Adamantidis. 2001. ''Use-dependent'' effects of cisapride on postrest action potentials in rabbit ventricular myocardium. *Eur. J. Pharmacol.* 422:137–148.
20. Swietach, P., C.-H. Leem, K. W. Spitzer, and R. D. Vaughan-Jones. 2005. Experimental generation and computational modeling of intracellular pH gradients in cardiac myocytes. *Biophys. J.* 88:3018–3037.
21. Antzelevitch, C., and G. K. Moe. 1981. Electrotonically mediated delayed conduction and reentry in relation to ''slow responses'' in mammalian ventricular conducting tissue. *Circ. Res.* 49:1129–1139.
22. Mitsuiye, T., and A. Noma. 1987. A new oil-gap method for internal perfusion and voltage clamp of single cardiac cells. *Pfluegers Arch.* 410:7–14.
23. Li, X., and P. C. H. Li. 2005. Microfluidic selection and retention of a single cardiac myocyte, on-chip loading, cell contraction by chemical stimulation, and quantitative fluorescent analysis of intracellular calcium. *Anal. Chem.* 77:4315–4322.
24. Riemer, T. L., and L. Tung. 2000. Focal extracellular potential: a means to monitor electrical activity in single cardiac myocytes. *Am. J. Physiol.* 278:H1383–H1394.